Journal of Cardiovascular Computed Tomography 16 (2022) 336–342

Contents lists available at ScienceDirect

Journal of Cardiovascular Computed Tomography

journal homepage: www.JournalofCardiovascularCT.com

Research paper

Diagnostic concordance and discordance between angiography-based quantitative flow ratio and fractional flow reserve derived from computed tomography in complex coronary artery disease

Hideyuki Kawashima [a,b,c], Norihiro Kogame [b], Masafumi Ono [a,b], Hironori Hara [a,b], Kuniaki Takahashi [b], Johan H.C. Reiber [d], Brian Thomsen [e], Robbert J. de Winter [b], Kaoru Tanaka [f], Mark La Meir [f], Johan de Mey [f], Ulrich Schneider [g], Torsten Doenst [g], Ulf Teichgräber [g], William Wijns [a,h], Saima Mushtaq [i], Giulio Pompilio [i,j], Antonio L. Bartorelli [i,k], Daniele Andreini [i,l], Patrick W. Serruys [a,h,m,*], Yoshinobu Onuma [a,h]

[a] Discipline of Cardiology, Saolta Group, Galway University Hospital, Health Service Executive and CORRIB Core Lab, National University of Ireland Galway (NUIG), Galway, Ireland
[b] Department of Cardiology, Academic Medical Centre, University of Amsterdam, Amsterdam, the Netherlands
[c] Division of Cardiology, Department of Internal Medicine, Teikyo University Hospital, Tokyo, Japan
[d] Department of Radiology, Leiden University Medical Center, Leiden, the Netherlands
[e] GE Healthcare, Milwaukee, WI, USA
[f] Universitair Ziekenhuis Brussel, VUB, Brussels, Belgium
[g] Jena University Hospital, Friedrich-Schiller-University of Jena, Jena, Germany
[h] CÚRAM, The SFI Research Centre for Medical Devices, Galway, Ireland
[i] Centro Cardiologico Monzino, IRCCS, Milan, Italy
[j] Department of Biomedical, Surgical and Dental Sciences, University of Milan, Milan, Italy
[k] Department of Biomedical and Clinical Sciences "Luigi Sacco", University of Milan, Milan, Italy
[l] Department of Clinical Sciences and Community Health, Cardiovascular Section, University of Milan, Milan, Italy
[m] NHLI, Imperial College London, London, United Kingdom

ARTICLE INFO

Keywords:
Quantitative flow ratio
Fractional flow reserve derived from computed tomography angiography
Multivessel disease
Coronary artery disease
SYNTAX score

ABSTRACT

Background: Both quantitative flow ratio (QFR) and fractional flow reserve derived from computed tomography (FFR_{CT}) have shown significant correlations with invasive wire-based fractional flow reserve. However, the correlation between QFR and FFR_{CT} is not fully investigated in patients with complex coronary artery disease (CAD). The aim of this study is to investigate the correlation and agreement between QFR and FFR_{CT} in patients with de novo three-vessel disease and/or left main CAD.

Methods: This is a post-hoc sub-analysis of the international, multicenter, and randomized SYNTAX III REVOLUTION trial, in which both invasive coronary angiography and coronary computed tomography angiography were prospectively obtained prior to the heart team discussion. QFR was performed in an independent core laboratory and compared with FFR_{CT} analyzed by HeartFlow™. The correlation and agreement between QFR and FFR_{CT} were assessed per vessel. Furthermore, independent factors of diagnostic discordance between QFR and FFR_{CT} were evaluated.

Results: Out of 223 patients, 40 patients were excluded from this analysis due to the unavailability of FFR_{CT} and/or QFR, and a total of 469 vessels (183 patients) were analyzed. There was a strong correlation between QFR and FFR_{CT} ($R = 0.759$; $p < 0.001$), and the Bland-Altman analysis demonstrated a mean difference of −0.005 and a standard deviation of 0.116. An independent predictor of diagnostic concordance between QFR and FFR_{CT} was the lesion location in right coronary artery (RCA) (odds ratio 0.395; 95% confidence interval 0.174–0.894; $P = 0.026$).

Conclusion: In patients with complex CAD, QFR and FFR_{CT} were strongly correlated. The location of the lesion in RCA was associated with the highest diagnostic concordance between QFR and FFR_{CT}.

* Corresponding author. Established Professor of Interventional Medicine and Innovation, National University of Ireland, Galway (NUIG), Galway, Ireland.
E-mail address: patrick.w.j.c.serruys@gmail.com (P.W. Serruys).

https://doi.org/10.1016/j.jcct.2022.02.004
Received 26 June 2021; Received in revised form 28 January 2022; Accepted 9 February 2022
Available online 19 February 2022

1. Introduction

Physiological assessment of coronary artery disease (CAD) has become one of the most important factors in decision making for myocardial revascularization.[1] There are two important binary decision points in the evaluation and management of patients with known or suspected CAD: first, to perform invasive coronary angiography (ICA), and second, to revascularize an identified coronary stenosis.[2] In the European Society of Cardiology (ESC) and American College of Cardiology/American Heart Association guidelines, fractional flow reserve (FFR) to guide revascularization as is a Class Ia recommendation[3,4]. Furthermore, the current ESC guidelines for chronic coronary syndrome (CCS) recommend the use of invasive FFR for localization of ischemia in multivessel CAD patients with angina symptoms even in cases, in which pre-procedural documentation of ischemia by non-invasive tests, such as echocardiography, stress echocardiography, myocardial perfusion imaging, or stress magnetic resonance imaging are available.[5]

Image derived physiological assessment, such as fractional flow reserve derived from computed tomography angiography (FFR_{CT}) and quantitative flow ratio (QFR), has also been developed. Non-invasive FFR_{CT} may provide anatomic information and functional evaluation of ischemia prior to ICA. A number of trials have demonstrated that the correlation between FFR_{CT} and invasive FFR is high[6,7,8]. Furthermore, FFR_{CT} has demonstrated its feasibility and accuracy even in patients with complex CAD.[9] Once ICA has been performed, QFR, which is a novel physiological assessment technique for the rapid computation of FFR, could be used.[10] QFR estimates the *trans*-stenotic pressure drop according to 3-dimensional (3D) quantitative coronary angiography (QCA) and virtual hyperemic flow derived from contrast frame count without real drug-induced hyperemia.[11] QFR improves the diagnostic accuracy by identifying hemodynamically significant lesions compared with the assessment of coronary stenosis on 2-dimensional QCA.[12,13] In addition, among patients with complex CAD, the diagnostic performance of QFR to predict binary wire-based ischemia has also been demonstrated.[14]

A previous study has demonstrated that FFR_{CT} and QFR were strongly correlated with invasive FFR in CCS population with relatively simple coronary lesions; however, diagnostic discordances between FFR_{CT} and FFR and between QFR and FFR were frequent.[15] The aim of the present sub-analysis of the SYNTAX III REVOLUTION trial[9] was to investigate the correlation and agreement between FFR_{CT} and QFR in patients with de novo three-vessel disease (3VD) and/or left main coronary artery disease (LMCAD).

2. Methods

2.1. Study design and population

The present study is a post-hoc analysis of the SYNTAX III REVOLUTION trial (NCT02813473), which has investigated the agreement in decision making between two heart teams on the selection of coronary artery bypass graft (CABG) or percutaneous coronary intervention (PCI) as modalities of revascularization, using either coronary computed tomography angiography (CCTA) with FFR_{CT} or ICA, while blinded to the other imaging modality in patients with de novo 3VD and/or LMCAD.[9] The details of protocol and main results of the trial were reported elsewhere.[9,16] The trial enrolled a total of 223 patients in 6 centers from five European countries. ICA was available for all patients. FFR_{CT} was available for 196/223 (87.9%) patients.[9] In the independent core laboratory (CORRIB Core Lab, Galway, Ireland), QFR was analyzed in those patients. Similarly, severity and extension of CAD were assessed using the anatomical SYNTAX score with CCTA and ICA.[17,18] The presence/absence of LMCAD was judged according to the calculation of the anatomical SYNTAX score derived from ICA.

The trial was approved by the investigational review board or ethics committee at each participating center. The principal investigators had unrestricted access to the data, were involved in the analysis and interpretation of the data. The principal investigators guarantee the completeness and accuracy of the data and analyses and the fidelity of the trial to the protocol.

2.2. Image acquisition and analysis of CCTA

CCTA was performed with the Revolution CT scanner (GE Healthcare, Milwaukee, WI, USA) that has a nominal spatial resolution of 230 μm along the X–Y planes, a rotational speed of 0.28 s and a Z-plane coverage of 16 cm enabling imaging of the whole heart in one heartbeat.[19] In select cases, a proprietary post-processing algorithm (SnapShot Freeze, GE Healthcare) was additionally used for the correction of any residual motion artefacts.[19] The protocol mandated the use of nitrates prior to CT acquisition and beta-blockers in cases of heart rate higher than 65 bpm.

2.3. Analysis of FFR_{CT}

The FFR_{CT} analysis was performed in a blinded fashion at the core laboratory (HeartFlow, Redwood City, California). FFR_{CT} was calculated from CCTA datasets by using computational fluid dynamics modeling after semiautomated segmentation of coronary arteries and left ventricular mass. Coronary blood flow and pressure were simulated under conditions modeling maximal hyperemia. Details of the underlying principle of FFR_{CT} computation were previously reported[6,20]. The continuous results of FFR_{CT} were displayed, color-coded and superimposed on the coronary arterial tree. $FFR_{CT} \leq 0.50$ was noted as $FFR_{CT} = 0.50$ because FFR_{CT} cannot provide actual values if ≤ 0.50. In case of total occlusion, FFR_{CT} was not provided but was regarded as $FFR_{CT} = 0.50$.[15] A cutoff $FFR_{CT} \leq 0.80$ was used to indicate a flow-limiting lesion.[21]

2.4. Image acquisition and analysis of QFR

In the SYNTAX III REVOLUTION trial, all ICA's were preceded by an intra-coronary injection of isosorbide dinitrate or nitroglycerin. In the independent core laboratory (CORRIB Core Lab, Galway, Ireland), offline QFR analysis was performed in a blinded fashion by experienced observers using validated software (QAngio XA 3D/QFR 1.0 software, Medis Medical Imaging Systems BV, Leiden, The Netherlands). Details of the QFR calculation method was reported previously.[10] In brief, QFR calculation was based on the 3D-QCA reconstruction derived from two angiographic projections with angles $\geq 25^{\circ}$ apart and volumetric flow rate calculated by using contrast bolus frame count.[12] QFR value was computed by applying contrast QFR without pharmacological hyperemic condition for the analysis.[12] Lesions were excluded from the analysis if they 1) had a reference lumen diameter below 2.0 mm by visual assessment, 2) presented slow coronary blood flow (Thrombolysis in Myocardial Infarction [TIMI] 1 or 2, 3) were acquired from less than two projections with isocenter calibration information, 4) had severe vessel overlap at the stenotic segments, or 5) had poor angiographic image quality precluding precise contour delineation.

QFR calculation was performed from the ostium of the main coronary vessels (i.e., right coronary artery [RCA], left main trunk [LM]/left anterior descending artery [LAD], and LM/left circumflex artery [LCX]) to the distal point with an anatomical landmark (i.e. side branch), at a site where the lumen diameter of the vessel was still at least 2 mm (Fig. 1).[14,22] In case of a LM lesion, the proximal point of analysis was set at the catheter tip. Because QFR cannot be measured in a totally occluded artery before revascularization, a default QFR value of 0.50 was imputed in the case of total or subtotal occlusions.[23] The automatic reference interpolation function was used to establish the reference diameter for QFR calculation. A cutoff $QFR \leq 0.80$ was used to indicate a flow-limiting lesion.[13] Reference vessel diameter, lesion length and percent area stenosis were derived from the 3D-QCA and displayed simultaneously with the QFR results.

2.5. Endpoints and statistical analysis

Quantitative variables are reported as mean ± standard deviation [SD] or median and interquartile range (interquartile range, 25–75%). Categorical variables are expressed as numeric values and percentages. The Pearson correlation and the Passing-Bablok regression analysis were used to quantify the correlation between QFR and FFR_{CT}.[24] Agreement between QFR and FFR_{CT} was assessed by the Bland-Altman plot.[25] Those analyses were preformed per vessel. Diagnostic discordance between QFR (≤0.80: positive or >0.80: negative) and FFR_{CT} (≤0.80: positive or >0.80: negative) was also assessed per vessel (Fig. 1). To assess factors of diagnostic discordance between QFR and FFR_{CT}, multivariate logistic regression analysis was conducted. Since a vessel level analysis was performed in the present study, the covariates in the adjusted model included the main coronary vessels (RCA, LM/LAD, or LM/LCX), the presence of lesion length >20 mm, heavy calcification, aorto-ostial lesion, and bifurcation or trifurcation in the vessel based on anatomical SYNTAX score calculation derived from ICA measured by the core laboratory, which had been selected based on prior knowledge of the association of these covariates with the outcomes.[26] In addition, since the data of QFR for LMCAD are not fully investigated, the correlation and agreement between QFR and FFR_{CT} in LAD and LCX stratified by the presence/absence of LMCAD were assessed. A 2-sided p-value <0.05 was considered to be statistically significant. All data were processed using SPSS version 26.0 (IBM Inc, Armonk, NY, USA).

3. Results

3.1. Study participants and baseline characteristics

Out of 223 patients in the SYNTAX III REVOLUTION trial, 27 (12.1%) patients were excluded from this analysis due to the unavailability of FFR_{CT}. Out of 596 vessels in 196 patients, 127 (21.3%) vessels were non-analyzable for QFR mainly due to no appropriate two projections (Fig. 2). Therefore, in the present study, a total of 469 (78.7%) vessels in 183 patients were analyzed.

Baseline patient characteristics are shown in Table 1, and vessel characteristics are presented in Table 2. Most patients were male, and the

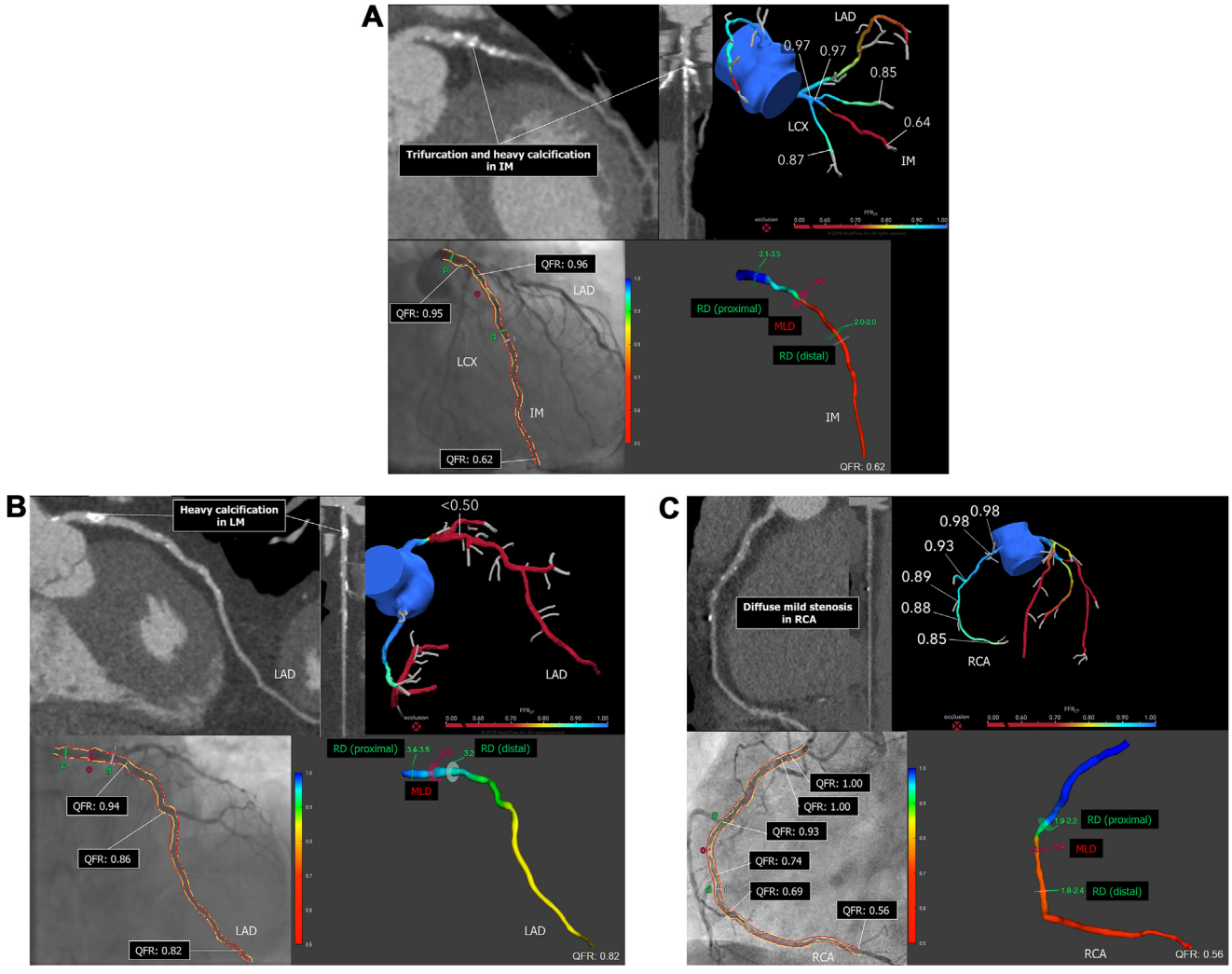

Fig. 1. Diagnostic concordance and discordance between FFR_{CT} and QFR. (A) Diagnostic concordance between FFR_{CT} and QFR. Top left panel: Curved MPR and straight MPR images in IM. Top right panel: FFR_{CT} analysis in IM. Bottom panel: QFR analysis (LM to IM). (B) Diagnostic discordance between FFR_{CT} and QFR (Positive FFR_{CT} and negative QFR). Top left panel: Curved MPR and straight MPR images in LAD. Top right panel: FFR_{CT} analysis in LAD. Bottom panel: QFR analysis (LM to LAD). (C) Diagnostic discordance between QFR and FFR_{CT} (Negative FFR_{CT} and positive QFR). Top left panel: Curved MPR and straight MPR images in RCA. Top right panel: FFR_{CT} analysis in RCA. Bottom panel: QFR analysis (RCA).
FFR_{CT}: fractional flow reserve derived from computed tomography; QFR: Quantitative flow ratio; MPR: multiplanar reconstruction; IM: intermediate artery; RCA: right coronary artery; LM: left main trunk; LAD: left descending artery; LCX: left circumflex; RD: reference diameter; MLD: minimum lumen diameter.

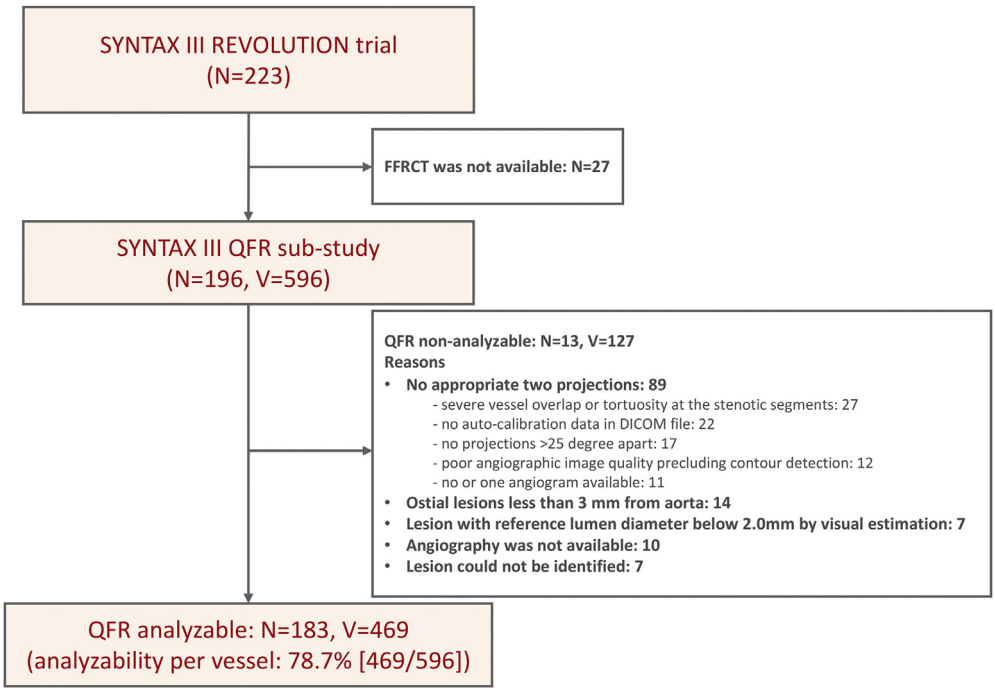

Fig. 2. Flowchart.
MSCT: multislice computed tomography; FFR_{CT}: fractional flow reserve derived from computed tomography; QFR: Quantitative flow ratio.

prevalence of diabetes mellitus was 36.0%. About one-fourth (25.7%) of patients had a LMCAD. Total occlusion was present in 20.5% (96/469) of vessels.

3.2. Correlation and agreement between QFR and FFR_{CT}

The correlation and agreement between QFR and FFR_{CT} are shown in Fig. 3 and Fig. 4.

Diagnostic discordance between QFR and FFR_{CT} was observed in 55 (11.7%) vessels and mainly occurred in vessels with high QFR (>0.80) and low FFR_{CT} (≤0.80) (Fig. 3). The Pearson correlation and the Passing-Bablok regression analysis demonstrated a strong positive correlation between QFR and FFR_{CT} (R = 0.759; 95% confidence interval [CI] 0.714 to 0.798; P < 0.001) (Fig. 3). The Bland-Altman analysis between QFR and FFR_{CT} demonstrated slightly lower value in FFR_{CT} with a mean difference of −0.005 and a SD of 0.116 (Fig. 4).

Table 1
Baseline characteristics of study patients.

Patient, number (%) or mean ± standard deviation	183 (100)
Male	159 (86.9)
Age, year-old	67.0 ± 8.9
Body mass index, kg/m^2	26.4 ± 3.6
Smoking	122 (63.2)
Past smoker	73 (41.2)
Current smoker	39 (22.0)
Diabetes mellitus	66 (36.0)
Type 1	7 (3.8)
Type 2	43 (32.2)
Insulin user	17 (9.4)
Hypertension	133 (72.7)
Hyperlipidemia	121 (66.1)
Previous stroke	15 (8.2)
Previous myocardial infarction	2 (1.1)
Previous cardiac surgery	0 (0)
COPD	21 (11.5)
Peripheral vascular disease	26 (14.2)
Creatinine clearance, ml/min	81.8 ± 27.8
Left ventricular ejection fraction, %	54.5 ± 11.3
Left main disease	47 (25.7)
Anatomical SYNTAX score derived from ICA measured by the core laboratory	29.6 ± 11.8
Anatomical SYNTAX score derived from MSCT measured by the core laboratory	33.3 ± 13.2

COPD: chronic obstructive pulmonary disease, ICA: invasive coronary artery disease, MSCT: multislice computed tomography.

Table 2
Baseline characteristics of study vessels.

Vessel, number (%) or mean ± standard deviation	469 (100)
RCA	136 (29.0)
LM/LAD	190 (40.5)
LM/LCX	143 (30.5)
Total occlusion	96 (20.5)
Bifurcation	126 (26.9)
Type of bifurcation	
Medina 1,0,0	12 (2.3)
Medina 0,1,0	15 (3.2)
Medina 1,1,0	21 (4.5)
Medina 1,1,1	41 (8.7)
Medina 0,0,1	14 (3.0)
Medina 1,0,1	12 (2.3)
Medina 0,1,1	11 (2.3)
Trifurcation	11 (2.3)
Aorto-ostial lesion	19 (4.1)
Severe tortuosity	7 (1.5)
Lesion length >20 mm	109 (23.2)
Heavy calcification[a]	77 (16.4)
Reference lumen diameter, mm	2.75 ± 0.64
FFR_{CT} ≤0.80	394 (84.0)
QFR ≤0.80	372 (79.3)

RCA: right coronary artery, LM: left main trunk; LAD: left descending artery, LCX: left circumflex, FFR_{CT}: fractional flow reserve derived from computed tomography, QFR: quantitative flow ratio, CCTA: coronary computed tomography angiography, ICA: invasive coronary angiography.

[a] On CCTA, heavy calcification was defined as presence of calcium that encompasses more than 50% of the cross-sectional area of the vessel at any location within the specific lesion.[9] On ICA, it was defined as multiple persisting opacifications of the coronary wall visible in more than one projection surrounding the complete lumen of the coronary artery at the site of the lesion.[9]

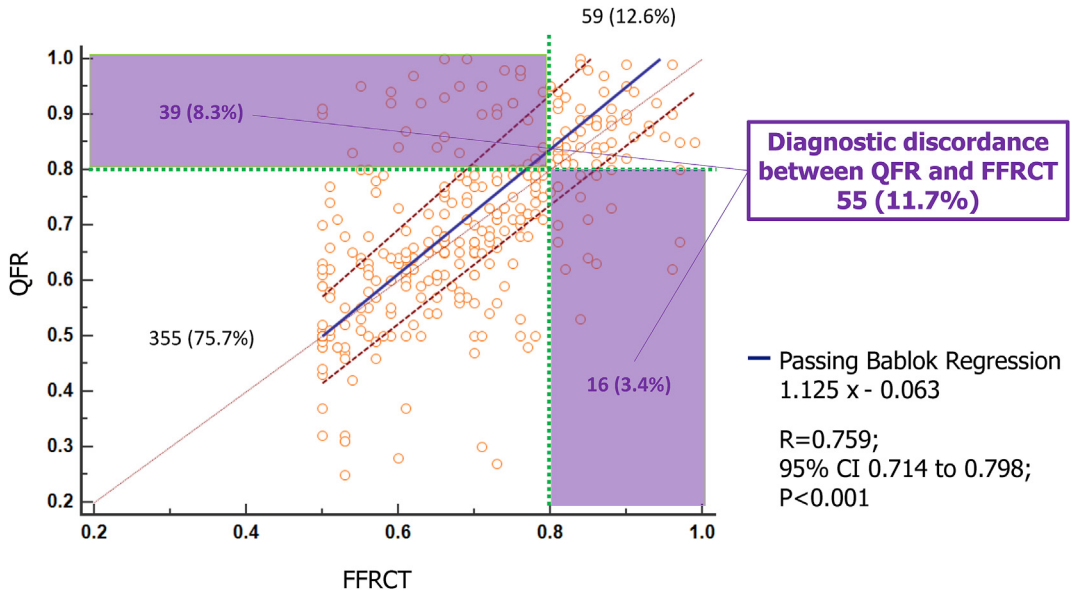

Fig. 3. Correlation between QFR and $FFR_{CT.}$
Scatter diagram with regression line between QFR and $FFR_{CT.}$ Blue line shows the regression line, and the red dotted lines show the 95% CI. The diagnostic discordance (55 vessels, 11.7%) is a total of QFR ≤0.80 and FFR_{CT} >0.80 (16 vessels, 3.4%) and FFR_{CT} ≤0.80 and QFR >0.80 (39 vessels, 8.3%).
QFR: Quantitative flow ratio; FFR_{CT}: fractional flow reserve derived from computed tomography; CI confidence interval. (For interpretation of the references to color in this figure legend, the reader is referred to the Web version of this article.)

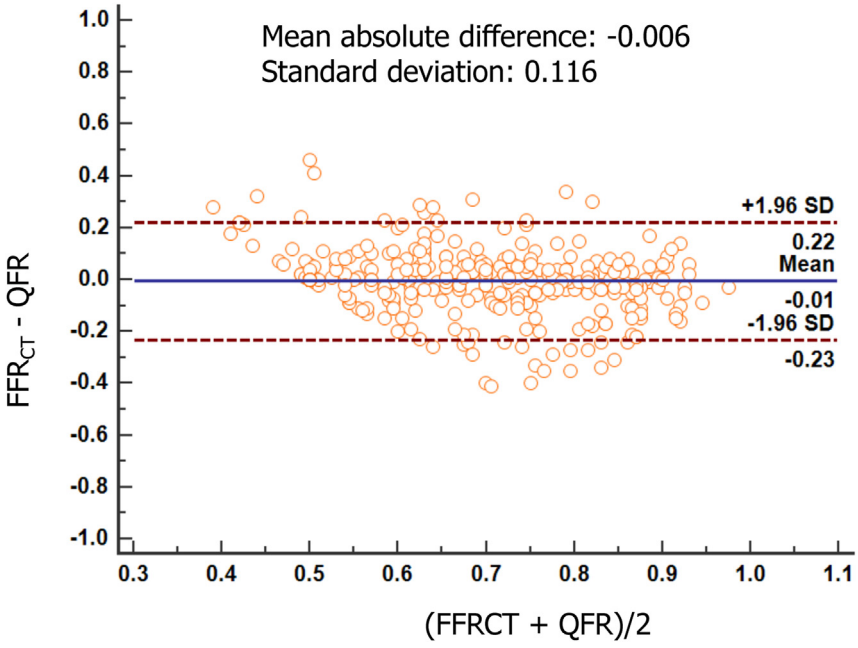

Fig. 4. Agreement between QFR and $FFR_{CT.}$
Bland-Altman plots of QFR and FFR_{CT}. Blue line shows the regression line, and the red dotted lines show the 95% CI.
QFR: Quantitative flow ratio; FFR_{CT}: fractional flow reserve derived from computed tomography; CI confidence interval. (For interpretation of the references to color in this figure legend, the reader is referred to the Web version of this article.)

3.3. Multivariate analysis to search for independent factors for diagnostic discordance between QFR and FFR_{CT}

The logistic regression analysis to investigate independent factors of diagnostic discordance between QFR and FFR_{CT} is shown in Table 3.

In the multivariate analysis, an independent predictor of diagnostic concordance between QFR and FFR_{CT} was the lesion location in RCA (odds ratio [OR] 0.395; 95% CI 0.174 to 0.894; P = 0.026). The other lesion characteristics such as heavy calcification were not independent predictors of the discordance between the two imaging modalities (OR 1.245; 95% CI 0.598 to 2.592; P = 0.557).

3.4. Correlation and agreement between QFR and FFR_{CT} in LAD and LCX stratified according to the presence/absence of LMCAD

When the vessels with LMCAD were included in the analysis, the Pearson correlation and the Passing-Bablok regression analysis demonstrated a strong positive correlation between QFR and FFR_{CT} in LM/LAD and LM/LCX (R = 0.709; 95% confidence interval [CI] 0.644 to 0.763; P < 0.001) (Online Fig. 1). The Bland-Altman analysis between QFR and FFR_{CT} in LM/LAD and LM/LCX demonstrated slightly lower value in FFR_{CT} with a mean difference of −0.010 and a SD of 0.125 (Online Fig. 1).

Table 3
Multivariate analysis to search for independent factors for diagnostic discordance between QFR and FFR_{CT}.

	Diagnostic discordance between QFR and FFR_{CT}	
	Odds ratio (95% CI)	P value
Vessel		
LM/LAD	Reference	–
RCA	0.395 (0.174–0.894)	0.026
LM/LCX	0.793 (0.411–1.530)	0.489
Lesion length >20 mm	0.559 (0.264–1.184)	0.129
Heavy calcification[a]	1.245 (0.598–2.592)	0.557
Aorto-ostial lesion	1.529 (0.475–4.918)	0.476
Bifurcation/trifurcation	1.328 (0.695–2.541)	0.391

QFR: quantitative flow ratio, FFR_{CT}: fractional flow reserve derived from computed tomography, LM: left main trunk; LAD: left descending artery, RCA: right coronary artery, LCX: left circumflex, CI: confidence interval.

[a] On CCTA, heavy calcification was defined as presence of calcium that encompasses more than 50% of the cross-sectional area of the vessel at any location within the specific lesion.[9] On ICA, it was defined as multiple persisting opacifications of the coronary wall visible in more than one projection surrounding the complete lumen of the coronary artery at the site of the lesion.[9]

When the vessels with LMCAD were not included in the analysis, the Pearson correlation and the Passing-Bablok regression analysis demonstrated a strong positive correlation between QFR and FFR_{CT} in LAD and LCX ($R = 0.794$; 95% confidence interval [CI] 0.735 to 0.841; $P < 0.001$) (Online Fig. 2). The Bland-Altman analysis between QFR and FFR_{CT} in LAD and LCX demonstrated slightly lower value in FFR_{CT} with a mean difference of −0.009 and a SD of 0.113 (Online Fig. 2).

4. Discussion

The main findings of the present study can be summarized as follows:

1. Among patients with de novo 3VD and/or LMCAD, QFR and FFR_{CT} were strongly correlated.
2. An independent predictor of diagnostic concordance between QFR and FFR_{CT} was the lesion location in RCA.
3. QFR and FFR_{CT} in LAD and LCX correlated well, regardless of the presence of LMCAD.

To the best of our knowledge, this is the first study to investigate the correlation and agreement between QFR and FFR_{CT} in a specific population of patients with de novo 3VD and/or LMCAD. Compared with invasive FFR, especially in patients with complex CAD, QFR and FFR_{CT} could reduce procedure time, wire-related complications, patient's discomfort and costs because there is no need to use a pressure guidewire or to induce maximum hyperemia. In the present sub-analysis of the SYNTAX III REVOLUTION trial, all patients had de novo 3VD and/or LMCAD with a mean angiographic anatomical SYNTAX score of 30.3 ± 12.2. Therefore, the heart team was consulted in the decision making on the revascularization treatment strategy to be followed, either CABG or PCI.[9] The main difference between this study and the study by Tanigaki et al.[15] is the absence or presence of invasive FFR as a comparator. However, in the present study, the mean diseased vessel number per patient was 2.6 (469 vessels/183 patients). This population represents a more anatomically complex CAD than the one enrolled in the previous publication by Tanigaki et al.,[15] in which the mean diseased vessel number per patient was 1.5 (233 vessels/152 patients).

In our analysis, heavy calcification and other complex lesion characteristics were not independent predictors of diagnostic discordance between QFR and FFR_{CT}. CCTA is sensitive in detecting calcium and its distribution, but the quantification of calcification is hampered and overestimated by the blooming artefact[27,28,29,30]. In the SYNTAX III REVOLUTION trial, heavily calcified lesions were documented in 28.9% according to the assessment of the heart team allocated to CCTA.[31] However, our results suggest that CCTA, especially when acquired with newest generation multislice computed tomography, could be used for patients with complex calcified lesions. In addition, a hypothetic explanation for better diagnostic concordance between QFR and FFR_{CT} in RCA compared to the other vessels is that the stenotic RCA might be less affected by heavy calcification from the aspects of anatomical factors and/or plaque components.

Especially for LMCAD, the diagnostic accuracy of QFR has not been fully evaluated.[32,33] To the best of our knowledge, the present study is the largest dataset including QFR analysis in LMCAD. In our analysis, LMCAD was included in one-fourth of patients. The exploratory analysis in LAD and LCX showed similar strong correlation between QFR and FFR_{CT} irrespective presence/absence of LMCAD. This finding may suggest the clinical relevance of QFR for LMCAD, although further trials comparing wire-based FFR and QFR are warranted.

Both FFR_{CT} and QFR could be used for decision making of revascularization mode, treatment planning, and possibly execution of PCI or CABG in the context of heart team discussion for patients with complex CAD. FFR_{CT} is used mainly in the outpatient setting and has been shown to reduce the number of unnecessary ICA in patients without functionally significant CAD.[34,35] In addition, CCTA with FFR_{CT} could be used for the decision making of heart team as demonstrated in the SYNTAX III REVOLUTION trial.[9] This imaging modality could provide the heart team with comprehensive information on anatomical disease extension, plaque composition, and physiological repercussion of narrowing. The ongoing FASTTRACK CABG trial is testing the feasibility and safety of treatment planning and execution of CABG solely based on CCTA and FFR_{CT}.[36] QFR obtained during diagnostic ICA helps the decision making in revascularization planning by identifying functionally significant lesions. In the SYNTAX II trial enrolling patients with 3VD, the percentage of analyzable QFR amounted to 71.0% of lesions, and QFR had a good correlation with the wire-based physiological assessment (area under the curve 0.81, accuracy 73.8%).[14] Furthermore, the post-procedural QFR after complex PCI had a significant prognostic impact on vessel oriented composite endpoint.[22] Kogame et al. demonstrated that the vessels with post-procedural QFR <0.91 had worse outcomes than those with post-procedural QFR ≥0.91.[22] Therefore, QFR could further guide PCI by providing functional assessment after stenting.

5. Limitations

The present study must be cautiously interpreted due to some limitations. First, invasive FFR as a gold standard of physiological assessment for intermediate coronary stenosis was not performed. However, a previous study demonstrated that QFR and FFR_{CT} showed a strong correlation with invasive FFR.[15] Therefore, we investigated factors of diagnostic discordance between QFR and FFR_{CT} on ischemia in patients with de novo 3VD and/or LMCAD. Second, the present study was a retrospective and non-pre-specified analysis. The ICA was not prospectively acquired according to specific acquisition protocol to fulfill all the technical requirement of QFR analysis. Third, the diagnostic performance of both QFR and FFR_{CT} in the scenario of concomitant epicardial and microvascular dysfunction and/or coronary collaterals to obstructed vessels was not investigated. In the presence of microvascular disease, there is an increase in the microvascular resistance resulting in reduced *trans*-stenotic pressure drop and flow values. In view of this, microvascular disease may impair the performance of both QFR and FFR_{CT} derived values. Indeed, the computational blood flow analysis of FFR_{CT} relies on the assumptions regarding microvascular resistance. Finally, FFR_{CT} and QFR are two "luminogram" surrogates of the pressure derived indices that were not available in this patient population. Ideally, the diagnostic accuracy of these two angiographic surrogates should be evaluated and compared with the gold standard of pressure measurement during hyperemia in the investigated population. Indeed, we relied on the validations on angiographic QFR and wire-based physiological assessment already reported in the literature and indulged ourselves in a comparison of surrogates.[14,22]

6. Conclusions

In patients with complex CAD, QFR and FFR_{CT} were strongly correlated. The location of the lesion in RCA was associated with the highest diagnostic concordance between QFR and FFR_{CT}.

Sources of funding

The SYNTAX III REVOLUTION trial was conducted under the support of the unrestricted resource from HeartFlow.

Trial registration number

NCT02813473.

Declaration of competing interest

Dr. Hara reports a grant for studying overseas from Japanese Circulation Society and a grant from Fukuda Foundation for Medical Technology, outside the submitted work.

Brian Thomsen is an employee of GE Healthcare.

Dr. Teichgräber reports grants from GE Healthcare, from null, outside the submitted work. Dr. Wijns reports grants and personal fees from MicroPort, outside the submitted work, and co-founder of Argonauts, an innovation facilitator.

Dr. Serruys reports personal fees from SMT, Philips/Volcano, Xeltis, Novartis, and Merillife.

All other authors have no conflict of interest to declare.

Acknowledgments

None.

Appendix A. Supplementary data

Supplementary data to this article can be found online at https://doi.org/10.1016/j.jcct.2022.02.004.

References

1. Kogame N, Ono M, Kawashima H, et al. The impact of coronary physiology on contemporary clinical decision making. *JACC Cardiovasc Interv*. 2020;13:1617–1638.
2. Hirshfeld Jr JW, Nathan ASQFR, Ffrct. Accurate enough? *JACC Cardiovasc Interv*. 2019;12:2060–2063.
3. Neumann FJ, Sousa-Uva M, Ahlsson A, et al. 2018 ESC/EACTS Guidelines on myocardial revascularization. *Eur Heart J*. 2019;40:87–165.
4. Patel MR, Calhoon JH, Dehmer GJ, et al. ACC/AATS/AHA/ASE/ASNC/SCAI/SCCT/STS 2017 appropriate use criteria for coronary revascularization in patients with stable ischemic heart disease: a report of the American College of Cardiology appropriate use criteria task force, American association for thoracic surgery, American heart association, American society of echocardiography, American society of nuclear Cardiology, society for cardiovascular angiography and interventions, society of cardiovascular computed tomography, and society of thoracic surgeons. *J Am Coll Cardiol*. 2017;69:2212–2241.
5. Knuuti J, Wijns W, Saraste A, et al. 2019 ESC Guidelines for the diagnosis and management of chronic coronary syndromes. *Eur Heart J*. 2020;41:407–477.
6. Koo BK, Erglis A, Doh JH, et al. Diagnosis of ischemia-causing coronary stenoses by noninvasive fractional flow reserve computed from coronary computed tomographic angiograms. Results from the prospective multicenter DISCOVER-FLOW (Diagnosis of Ischemia-Causing Stenoses Obtained via Noninvasive Fractional Flow Reserve) study. *J Am Coll Cardiol*. 2011;58:1989–1997.
7. Min JK, Leipsic J, Pencina MJ, et al. Diagnostic accuracy of fractional flow reserve from anatomic CT angiography. *JAMA*. 2012;308:1237–1245.
8. Norgaard BL, Leipsic J, Gaur S, et al. Diagnostic performance of noninvasive fractional flow reserve derived from coronary computed tomography angiography in suspected coronary artery disease: the NXT trial (Analysis of Coronary Blood Flow Using CT Angiography: next Steps). *J Am Coll Cardiol*. 2014;63:1145–1155.
9. Collet C, Onuma Y, Andreini D, et al. Coronary computed tomography angiography for heart team decision-making in multivessel coronary artery disease. *Eur Heart J*. 2018;39:3689–3698.
10. Tu S, Barbato E, Koszegi Z, et al. Fractional flow reserve calculation from 3-dimensional quantitative coronary angiography and TIMI frame count: a fast computer model to quantify the functional significance of moderately obstructed coronary arteries. *JACC Cardiovasc Interv*. 2014;7:768–777.
11. Westra J, Andersen BK, Campo G, et al. Diagnostic performance of in-procedure angiography-derived quantitative flow reserve compared to pressure-derived fractional flow reserve: the FAVOR II europe-Japan study. *J Am Heart Assoc*. 2018;7.
12. Tu S, Westra J, Yang J, et al. Diagnostic accuracy of fast computational approaches to derive fractional flow reserve from diagnostic coronary angiography: the international multicenter FAVOR pilot study. *JACC Cardiovasc Interv*. 2016;9:2024–2035.
13. Xu B, Tu S, Qiao S, et al. Diagnostic accuracy of angiography-based quantitative flow ratio measurements for online assessment of coronary stenosis. *J Am Coll Cardiol*. 2017;70:3077–3087.
14. Asano T, Katagiri Y, Chang CC, et al. Angiography-derived fractional flow reserve in the SYNTAX II trial: feasibility, diagnostic performance of quantitative flow ratio, and clinical prognostic value of functional SYNTAX score derived from quantitative flow ratio in patients with 3-vessel disease. *JACC Cardiovasc Interv*. 2019;12:259–270.
15. Tanigaki T, Emori H, Kawase Y, et al. QFR versus FFR derived from computed tomography for functional assessment of coronary artery stenosis. *JACC Cardiovasc Interv*. 2019;12:2050–2059.
16. Cavalcante R, Onuma Y, Sotomi Y, et al. Non-invasive Heart Team assessment of multivessel coronary disease with coronary computed tomography angiography based on SYNTAX score II treatment recommendations: design and rationale of the randomised SYNTAX III Revolution trial. *EuroIntervention*. 2017;12:2001–2008.
17. Serruys PW, Onuma Y, Garg S, et al. Assessment of the SYNTAX score in the Syntax study. *EuroIntervention*. 2009;5:50–56.
18. Collet C, Miyazaki Y, Ryan N, et al. Fractional flow reserve derived from computed tomographic angiography in patients with multivessel CAD. *J Am Coll Cardiol*. 2018;71:2756–2769.
19. Andreini D, Pontone G, Mushtaq S, et al. Image quality and radiation dose of coronary CT angiography performed with whole-heart coverage CT scanner with intra-cycle motion correction algorithm in patients with atrial fibrillation. *Eur Radiol*. 2017;28:1383–1392.
20. Serruys PW, Chichareon P, Modolo R, et al. The SYNTAX score on its way out or towards artificial intelligence: part I. *EuroIntervention*. 2019;16:44–59.
21. Patel MR, Norgaard BL, Fairbairn TA, et al. 1-Year impact on medical practice and clinical outcomes of FFRCT: the ADVANCE registry. *JACC Cardiovasc Imaging*. 2020;13:97–105.
22. Kogame N, Takahashi K, Tomaniak M, et al. Clinical implication of quantitative flow ratio after percutaneous coronary intervention for 3-vessel disease. *JACC Cardiovasc Interv*. 2019;12:2064–2075.
23. Tonino PA, De Bruyne B, Pijls NH, et al. Fractional flow reserve versus angiography for guiding percutaneous coronary intervention. *N Engl J Med*. 2009;360:213–224.
24. Passing H, Bablok. A new biometrical procedure for testing the equality of measurements from two different analytical methods. Application of linear regression procedures for method comparison studies in clinical chemistry, Part I. *J Clin Chem Clin Biochem*. 1983;21:709–720.
25. Bland JM, Altman DG. Statistical methods for assessing agreement between two methods of clinical measurement. *Lancet*. 1986;1:307–310.
26. Pocock SJ, McMurray JJV, Collier TJ. Statistical controversies in reporting of clinical trials: Part 2 of a 4-Part Series on statistics for clinical trials. *J Am Coll Cardiol*. 2015;66:2648–2662.
27. Zhang S, Levin DC, Halpern EJ, Fischman D, Savage M, Walinsky P. Accuracy of MDCT in assessing the degree of stenosis caused by calcified coronary artery plaques. *AJR Am J Roentgenol*. 2008;191:1676–1683.
28. Yan RT, Miller JM, Rochitte CE, et al. Predictors of inaccurate coronary arterial stenosis assessment by CT angiography. *JACC Cardiovasc Imaging*. 2013;6:963–972.
29. Li P, Xu L, Yang L, et al. Blooming artifact reduction in coronary artery calcification by A new de-blooming algorithm: initial study. *Sci Rep*. 2018;8:6945.
30. Kogame N, Serruys PW, Onuma Y. Cracking (the code of) coronary artery calcification to win the last battle of percutaneous coronary intervention: still in the middle of a rocky road. *Eur Heart J*. 2020;41:797–800.
31. Andreini D, Modolo R, Katagiri Y, et al. Impact of fractional flow reserve derived from coronary computed tomography angiography on heart team treatment decision-making in patients with multivessel coronary artery disease: insights from the SYNTAX III REVOLUTION trial. *Circ Cardiovasc Interv*. 2019;12, e007607.
32. Zhang R, Song C, Guan C, et al. Prognostic value of quantitative flow ratio based functional SYNTAX score in patients with left main or multivessel coronary artery disease. *Circ Cardiovasc Interv*. 2020;13, e009155.
33. Lopez-Palop R, Carrillo P, Leithold G, Frutos A, Pinar E, Freites A. Diagnostic accuracy of angiography-based quantitative flow ratio in patients with left main disease. *Rev Esp Cardiol*. 2020;74:357–359.
34. Norgaard BL, Hjort J, Gaur S, et al. Clinical use of coronary CTA-derived FFR for decision-making in stable CAD. *JACC Cardiovasc Imaging*. 2017;10:541–550.
35. Shiono Y, Matsuo H, Kawasaki T, et al. Clinical impact of coronary computed tomography angiography-derived fractional flow reserve on Japanese population in the ADVANCE registry. *Circ J*. 2019;83:1293–1301.
36. Kawashima H, Pompilio G, Andreini D, et al. Safety and feasibility evaluation of planning and execution of surgical revascularisation solely based on coronary CTA and FFRCT in patients with complex coronary artery disease: study protocol of the FASTTRACK CABG study. *BMJ Open*. 2020;10, e038152.